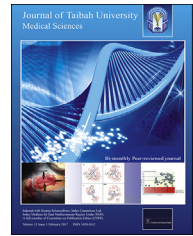




Taibah University

Journal of Taibah University Medical Sciences

www.sciencedirect.com



Original Article

Evaluation of antibacterial activity from phytosynthesized silver nanoparticles against medical devices infected with *Staphylococcus* spp.



Kumari Jyoti, MSc and Ajeet Singh, PhD*

Department of Biotechnology, Govind Ballabh Pant Engineering College, Pauri Garhwal, India

Received 20 May 2016; revised 5 August 2016; accepted 21 August 2016; Available online 27 September 2016

المخلص

أهداف البحث: تُعتبر التكوينات الحيوية الرقيقة والعدوى البكتيرية على سطح المعدات الطبية مثل الأطراف الاصطناعية وأنابيب القسطرة تحد خطير لعلم الطب الحيوي. فشلت أغلب الطرق التقليدية مثل العلاج بالمضادات الحيوية واستبدال المعدات الطبية بسبب ضعف فاعليتهم في البيئة الطبية. استهدفنا في هذه الدراسة منع الإصابة بالعدوى ببكتيريا ستافيلوكوكس إبيديميس (٣٥٩٨٤) وبكتيريا ستافيلوكوكس أوريوس (٧٤٠) المسببتين للأمراض والمعروفتين بأنهما سلالتان تشارك في إصابات بشرية ومقاومتان للعلاج بالمضادات الحيوية، وذلك باستخدام طلاء الجسيمات النانوية الفضية المصنعة نباتياً.

طرق البحث: تم تصنيع الجسيمات النانوية الفضية باستخدام المستخلص المائي لأوراق بيربرس أيشياتيكا، وتم تمييزها باستخدام جهاز التحليل الطيفي فوق البنفسجي، وجهاز حيود الأشعة السينية، وجهاز "فوريريه" لتحويل طيف الأشعة تحت الحمراء، والمجهر الإلكتروني المسحي، ومجهر القوة الذرية، والتحليل الطيفي المبني على تشتت الطاقة، والمجهر الإلكتروني الانتقالي وحيود الإلكترون لمنطقة محددة. وقد تم عد خلايا البكتيريا الحية باستخدام عداد المستعمرات الرقعي.

النتائج: أظهرت النتائج بأن الجسيمات النانوية الفضية كانت في المناطق الحجمي ٣٥-١٥ نانومتر، وكانت متبلورة على شكل بنية مكعبة مركزية الوجوه. إضافة إلى ذلك فإن طلاء الجسيمات النانوية الفضية على الأسطح الزجاجية تسبب في نشاط فاعل قاتل للبكتيريا.

الاستنتاجات: تشير هذه الدراسة إلى أن الجسيمات النانوية الفضية المصنعة نباتياً والمتوجة بجزيئات حيوية مختلفة موجودة في مستخلص أوراق بيربرس أيشياتيكا المطبلة على سطح زجاجي تساعد على منع عدوى المعدات الطبية ببكتيريا ستافيلوكوكس إبيديميس وبكتيريا ستافيلوكوكس أوريوس. وبذلك فإن طلاء الأسطح الزجاجية بالجسيمات النانوية الفضية المصنعة نباتياً قد يوفر عاملاً فاعلاً مضاداً للبكتيريا في علاج عدوى الجهاز الطبي.

الكلمات المفتاحية: الجسيمات النانوية الفضية؛ مجهر القوة الذرية؛ إتصاق البكتيريا؛ بيربرس أيشياتيكا؛ المجهر الإلكتروني الانتقالي

Abstract

Objectives: Biofilm formation on the surface of medical devices, such as artificial prosthetics and catheters, are serious challenges to biomedical science. Most conventional methods, such as antibiotic therapy and medical device replacement, have failed because of low efficiency in medical environments. In the present study, we aimed to prevent infection by human pathogens *Staphylococcus epidermidis* (35984) and *Staphylococcus aureus* (740), which are resistant to antibiotic therapy. To prevent these infections, phytosynthesized silver nanoparticles (AgNPs) coating was tested.

Methods: The AgNPs were synthesized using aqueous extract of *Berberis asiatica* leaves and were characterized by UV–vis spectroscopy, X-ray diffraction (XRD), Fourier transform infrared spectroscopy (FTIR), scanning electron microscopy (SEM), atomic force microscopy (AFM), energy dispersive spectroscopy (EDS), transmission electron microscopy (TEM), and selected area electron diffraction (SAED). The viable cells of bacteria were counted using a digital colony counter.

Results: AgNPs were 15 nm–35 nm in size and crystallized in a face-centred-cubic structure. Furthermore, the AgNPs coating on glass surfaces were bactericidal.

Conclusions: This study suggested that phytosynthesized AgNPs capped with various biomolecules present in leaf extracts of *B. asiatica* coated on glass surface prevent *S. epidermidis* and *S. aureus* associated infections of medical devices. Thus, coating of phytosynthesized AgNPs on glass surfaces may provide efficient antibacterial treatment of infected medical devices.

* Corresponding address: Department of Biotechnology, Govind Ballabh Pant Engineering College, Pauri Garhwal, 246194, Uttarakhand, India.

E-mail: ajeetsoniyal@gmail.com (A. Singh)

Peer review under responsibility of Taibah University.



Production and hosting by Elsevier

Keywords: AFM; AgNPs; Bacterial adhesion; *Berberis asiatica*; TEM

© 2016 The Authors.

Production and hosting by Elsevier Ltd on behalf of Taibah University. This is an open access article under the CC BY-NC-ND license (<http://creativecommons.org/licenses/by-nc-nd/4.0/>).

Introduction

Silver nanoparticles are important metal nano materials. Their larger surface-to-volume ratio, higher surface energy, and unique surface plasmon resonance (SPR) effects have a wide range of applications, including wound dressing, protective clothing, new nanomedicines, antibacterial surfaces, water treatment, food preservation and disinfecting agents.^{1–3} Conventional synthesis of silver nanoparticles includes physical methods using elevated temperatures and high pressures, as well as chemical methods using toxic chemicals that pollute the environment.⁴ Therefore, green synthesis approaches have been sought as valuable alternatives with many advantages, such as ecofriendliness, energy efficiency, non-toxicity, and compatibility with medical applications.^{5,6} Colonization, biofilm formation, and adherence of pathogenic bacteria on various human surfaces are associated with infections exhibit high resistances to available therapies.⁷ Infections associated with medical devices are becoming increasingly common among nosocomial infections due to high contamination of devices during use.^{8–10} Furthermore, infectious agents are serious challenges and can spread to other immune-privileged sites. The conventional antibacterial therapies have little or no effects against pathogenic biofilm populations colonised on medical devices. Replacement or surgical removal of the medical devices is often essential, and in certain cases, patients require intermittent antibiotic treatment for the rest of their lives where device removal is not a viable option.¹¹ Complications arising from biofilm infections lead to significant morbidity and mortality,¹² which necessitates identification of novel approaches to eliminate biofilm infections on medical devices. At present, various conventional strategies using standard antibacterial agents have been used ineffectively to treat and prevent biofilm formation. There are reports that green synthesized silver nanoparticles have efficient antimicrobial activities against bacteria, viruses, and other eukaryotic microorganisms.^{13,14} In addition, silver nanoparticles are also reported to possess anti-inflammatory¹⁵ and anti-angiogenic activity,¹⁶ which supports their applications for medical purposes.

Berberis asiatica is an important Ayurvedic medicinal plant, belonging to family Berberidaceae. In this study, *B. asiatica* leaves were extracted for synthesis of silver nanoparticles and were used to prevent biofilm formation on glass surfaces against. Strains tested included *Staphylococcus epidermidis* (35984) and *Staphylococcus aureus* (740), which is a well-known strain involved in human infections and resistant to commercially available antibiotics (e.g., gentamycin).^{17–19}

B. asiatica (Figure 1) is a pretty evergreen thorny shrub, measuring 1.8–2.4 m in height; these shrubs commonly occur on the dry outer Himalaya. Leaves are 2.5 cm–6.3 cm by 1.3 cm–3 cm long, usually elliptical with large distinct spines. This shrub has been traditionally used for its anti-inflammatory, antidiabetic, analgesic, antipyretic, diuretic, hepatoprotective, antimicrobial, antioxidant, strong wound healer, anti-rheumatic properties.^{20,21}

Materials and Methods

Plant and chemicals

The leaves of *B. asiatica* were collected from G.B. Pant Engineering College campus (Ghurdauri, Pauri, Uttarakhand, India). The sample taxonomy was authenticated by the department of Botany, Hemwati Nandan Bahuguna Garhwal University (Central University) Srinagar, Uttarakhand, India. Standard cultures of *S. epidermidis* (35984) for antibacterial assays were procured from American Type Culture Collection (ATCC) and *S. aureus* (740) was procured from Microbial Type Culture Collection (MTCC), IMTECH, Chandigarh, India.

Preparation of *Berberis asiatica* leaf extracts

B. asiatica leaves (20 g) were washed with Milli Q water, cut into small pieces, and boiled for 15 min in 250 ml Erlenmeyer flasks containing 100 ml Milli Q water. The extract was then filtered through Whatman filter paper No. 1 and stored at 4 °C till further use.²²

Synthesis of silver nanoparticles

To initiate the synthesis of AgNPs, 2.5 ml of leaf extracts were mixed with 47.5 ml of 1 mM silver nitrate (AgNO₃) solution with constant stirring for 10 min and kept for incubation at 40 °C for 60 min in the dark. AgNP formation was marked by a change in colour of the AgNO₃ aqueous solution from colourless to brown.



Figure 1: Leaves of *Berberis asiatica*.

Characterization of AgNPs

The phytosynthesized AgNPs were characterized by Ultraviolet–visible spectral analysis. The absorbance spectra were recorded using Ultraviolet–visible spectroscopy (UV-1800 Shimadzu UV spectrophotometer) from 300 to 700 nm. Fourier transform infrared spectroscopy was performed on a Thermo Scientific™ Nicolet iS™50 FTIR Spectrometer to detect possible functional groups in biomolecules present from leaf extracts of *B. asiatica*. X-ray diffraction was performed on a X-ray diffractometer (Panalytical Xpert-PRO 3050/60) operated at 30 kV and 100 mA and the spectrum was recorded by CuK α radiation with wavelength of 1.5406 Å in the 2θ range of 20°–80°. The surface morphology and size of the AgNPs were examined using a scanning electron microscope (SEM) on a NOVA-450 instrument. Transmission electron microscope (TEM), energy dispersive spectroscopy (EDS), and selected area electron diffraction (SAED) measurements were performed on a Tecnai G2 20 S-TWIN instrument. The atomic force microscopy (AFM) used a nanoscope8 in its non-contact mode. Viable bacteria cells were counted using a digital colony counter (LAB India).

Coating of AgNPs on glass surface

Glass slides were prepared by immersing them in a colloidal suspension of AgNPs (1 mg/ml) followed by incubation for 18 h at 25 °C. Next, glass slides were placed in a water bath sonicator for 10 min and air dried.²³

Antibacterial activity of glass coated with AgNPs

Antibacterial activity of glass coated with AgNPs was investigated against *S. epidermidis* and *S. aureus*, common pathogenic strains on medical devices as well as involved in human infections that are resistant to commercially available antibiotics. Overnight cultures were diluted with 0.9% NaCl to a 0.5% Mcfarland standard. The bacterial suspension (10 μ l) was deposited on a standard microscopic slide and subsequently covered with a glass slide coated with AgNPs to form a thin film between slides and facilitate direct contact of the bacterial with the AgNPs. The two glass slides were kept in an autoclaved petri plate containing 1 ml of phosphate buffer saline (PBS) to maintain a damp environment. The slides in contact with the liquid films containing bacteria were maintained at room temperature for 6 h, 10 h and 18 h,

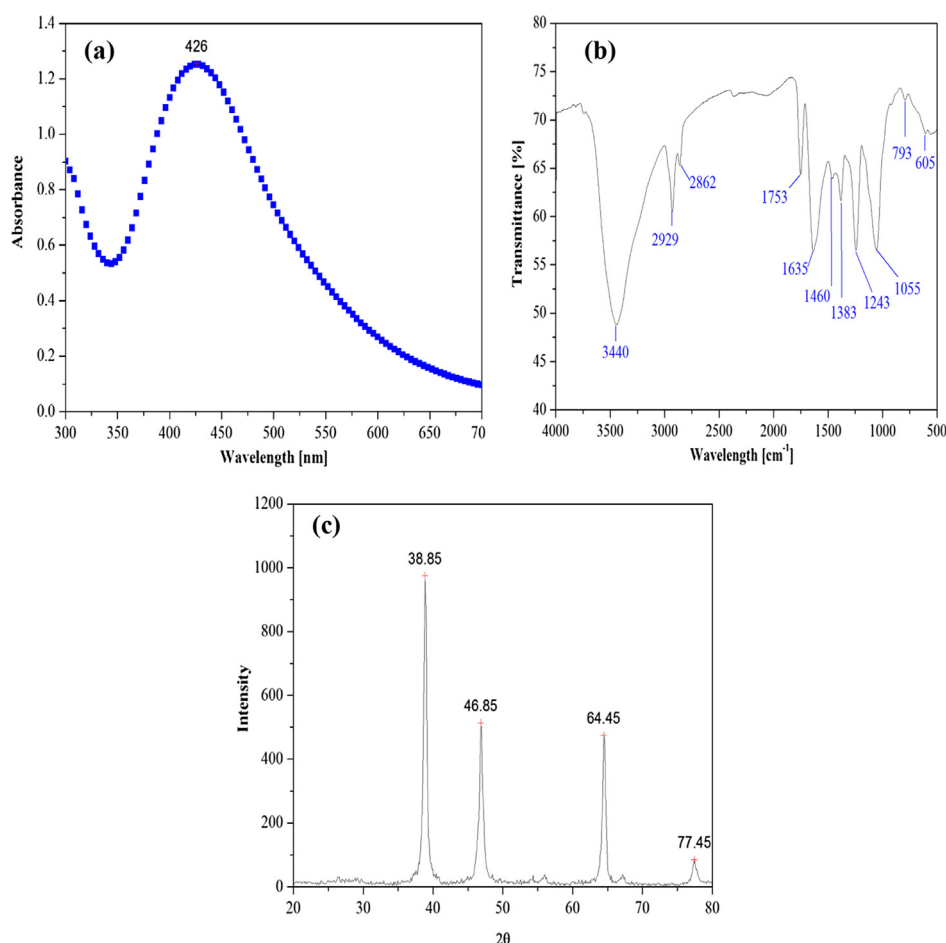


Figure 2: Characterization of phytosynthesized AgNPs from *Berberis asiatica*, where (a) UV–vis absorption spectrum, (b) FTIR spectrum, and (c) XRD pattern.

respectively; for each time of contact, an uncoated glass slide was treated the same way as a control. After the contact time, 9 ml of PBS was introduced in each autoclaved petriplate with gentle shaking to detach the assembled glass slides. Next, the bacterial suspension was grown in Nutrient agar medium to count viable cells. The bactericidal effect (BE) was calculated as

$$BE = \frac{\log N_C - \log N_E}{\log N_C}$$

where N_C is the number of Colony Forming Unit (CFU)/ml developed on control glass and N_E is the number of CFU/ml counted after exposure to AgNPs modified glass.²³

Statistical analysis

All experiments were performed in triplicate and student's *t*-test was used to evaluate statistically significant differences, where $p < 0.05$ was considered to be significant.

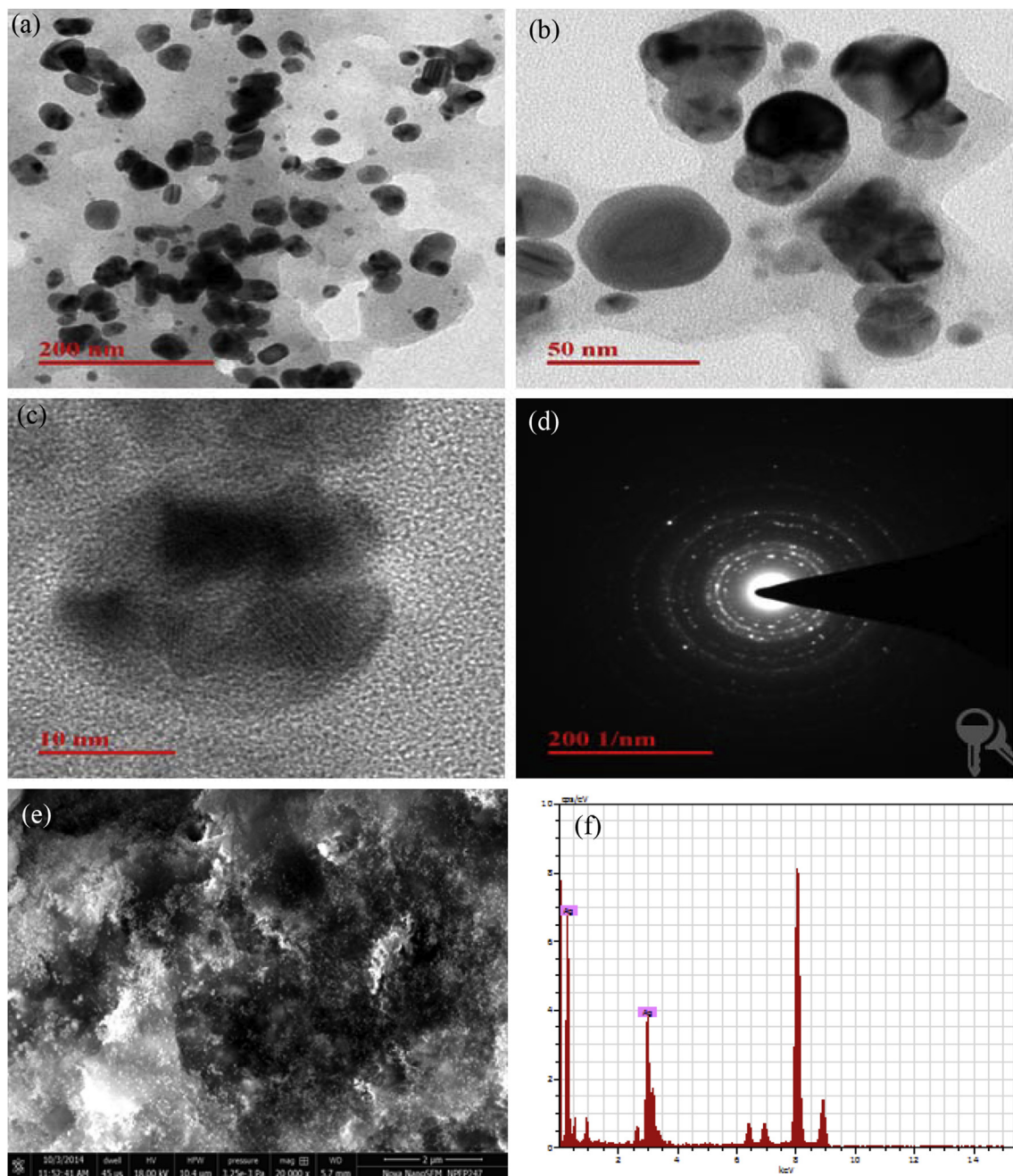


Figure 3: (a–c) TEM images of phytosynthesized AgNPs formed by reduction of Ag^+ ions using aqueous *Berberis asiatica* leaf extracts at 200 nm, 50 nm, and 10 nm scale, (d) SAED pattern of the AgNPs indicates that nanoparticles are highly crystalline, (e) SEM image of phytosynthesized AgNPs, (f) EDS of AgNPs.

Results

B. asiatica leaf extracts were used for the synthesis of AgNPs. The reduction of pure Ag to nanoparticles was monitored by UV–vis spectrum from 300 nm to 700 nm. The UV–visible spectra of AgNPs are shown in Figure 2a with well-defined surface plasmon bands centred approximately 426 nm. The SPR band depends upon the particles shape, size, and chemicals surrounding adsorbed species on the surface.²⁴ SPR is a collective excitation of the electrons in the conduction band around the nanoparticles surface. The formation of AgNPs was probably due to the reduction of Ag^+ ions into Ag^0 atoms by the *B. asiatica* leaf extracts added to the AgNO_3 solution.

The FTIR spectra of phytosynthesized AgNPs manifests absorption peak located near 3440 cm^{-1} , 2929 cm^{-1} , 2862 cm^{-1} , 1753 cm^{-1} , 1635 cm^{-1} , 1460 cm^{-1} , 1383 cm^{-1} , 1243 cm^{-1} , 1055 cm^{-1} , 793 cm^{-1} , and 605 cm^{-1} (Figure 2b). The synthesized AgNPs phase was measured by XRD as shown in Figure 2c. The presence of intense peaks at $2\theta = 38.85$, 46.85 , 64.85 , and 77.45 corresponds to planes of (1 1 1), (2 0 0), (2 2 0), and (3 1 1), respectively, which can be indexed according to the facets of silver.²⁵

The size determined by TEM analysis was found to be from 15 nm to 35 nm (Figure 3a–c). The AgNPs morphology was also studied by SEM (Figure 3e). Bright circular rings in the SAED pattern of AgNPs revealed their crystalline nature (Figure 3d). The elemental analysis of the AgNPs was performed using EDS. The EDS spectra of phytosynthesized AgNPs are shown in Figure 3f and show a strong peak at 3 KeV, which means that AgNPs are entirely composed of Ag.²⁶ Surface morphology and size of coated AgNPs synthesized from *B. asiatica* leaf extracts were further studied by AFM analysis and are shown in Figure 4a and b. The phytosynthesized AgNPs were found to be approximately 27 nm as was found previously by XRD and TEM studies.

To understand the inhibitory effect of AgNP coating to prevent bacterial adhesion, we assessed the bactericidal effect of glass coated with AgNPs in contact with liquid film of *S. epidermidis* and *S. aureus*. Bactericidal effect was calculated by growing bacterial suspensions of each sample in Nutrient

Table 1: Bactericidal effect of glass coated with AgNPs on *Staphylococcus epidermidis* and *Staphylococcus aureus* after 6 h, 10 h and 18 h of contact.

Contact time of AgNPs grafted on glass surface with liquid film of <i>Staphylococcus epidermidis</i> and <i>Staphylococcus aureus</i>			
Test pathogen	6 h	10 h	18 h
	Bactericidal effect (BE)		
<i>Staphylococcus epidermidis</i>	3.15 ± 0.01	3.29 ± 0.02	3.36 ± 0.01
<i>Staphylococcus aureus</i>	3.20 ± 0.02	3.35 ± 0.03	3.60 ± 0.01

agar media to count viable cells using a digital colony counter. In this study, we developed a practical test to prevent the bacterial adhesion by coating the glass surface layer with AgNPs and is in contact with liquid films of *S. epidermidis* and *S. aureus*. The phytosynthesized AgNPs showed stronger antibacterial effect against *S. epidermidis* and *S. aureus* (Table 1; Figures 5 and 6). The bactericidal effect due to the coated AgNPs on glass surfaces may prevent bacterial adhesion of pathogenic bacteria on medical devices.

Discussion

Bioresources, such as plants, are important sources of environmentally benign, bioactive compounds for nanoparticle production. In this study, a green chemistry approach was used to synthesize AgNPs using *B. asiatica* leaf extracts. The phytosynthesized AgNPs were further screened for antibiofilm activity against Gram-positive bacteria, *S. epidermidis* and *S. aureus*. When aqueous leaf extracts of *B. asiatica* were added to silver nitrate solution in the dark, the resultant solution turned dark brown, while no colour change was observed in the absence of plant extract incubated under the same conditions. The appearance of a dark brown colour in solution indicated the formation of AgNPs. A characteristic SPR peak at 426 nm in UV–vis spectrum was observed at 60 min of incubation at 40°C . Past studies suggested that a SPR peak located between 410 nm and 450 nm exists for AgNPs and might be attributed to spherical nanoparticles.²⁷ The stability of the phytosynthesized AgNPs was studied by

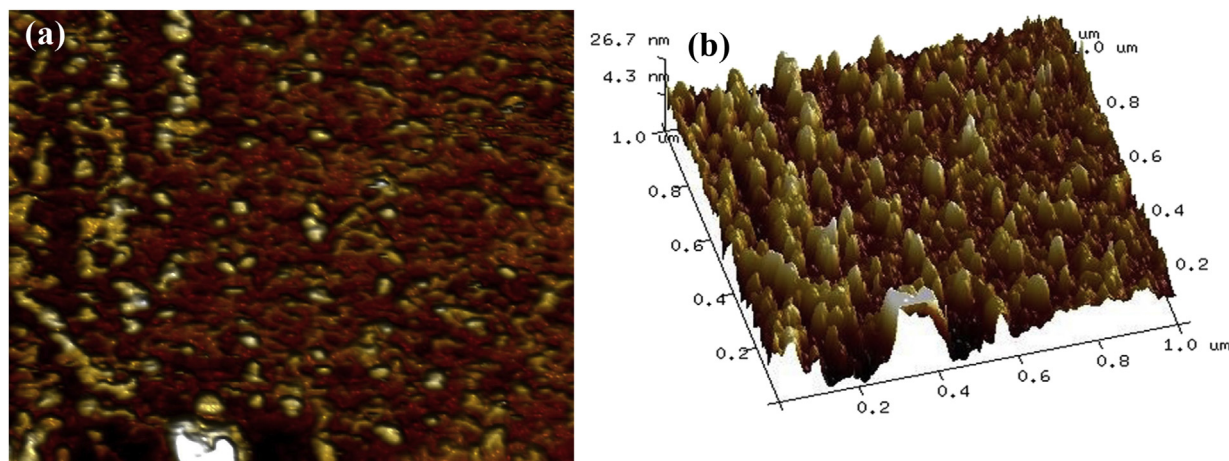


Figure 4: (a–b) AFM micrograph of coated AgNPs phytosynthesized using *Berberis asiatica* leaf extracts on glass surface.

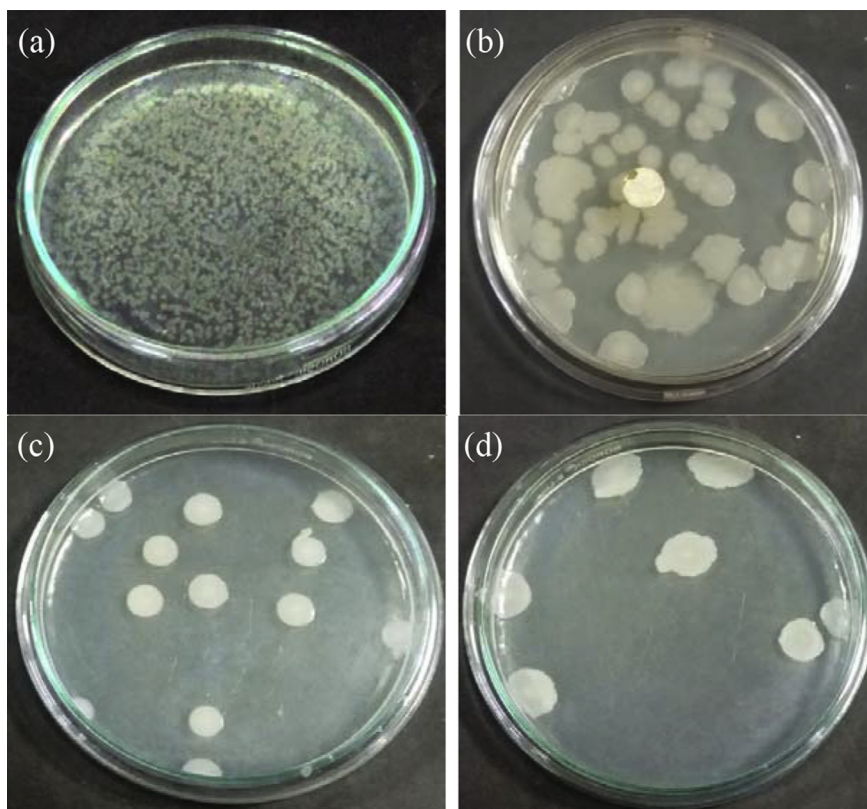


Figure 5: (a) Plate showing number of colonies of *Staphylococcus epidermidis* before treatment of AgNPs, (b) After 6 h of treatment with AgNPs, (c) After 10 h of treatment with AgNPs, (d) After 18 h of treatment with AgNPs.

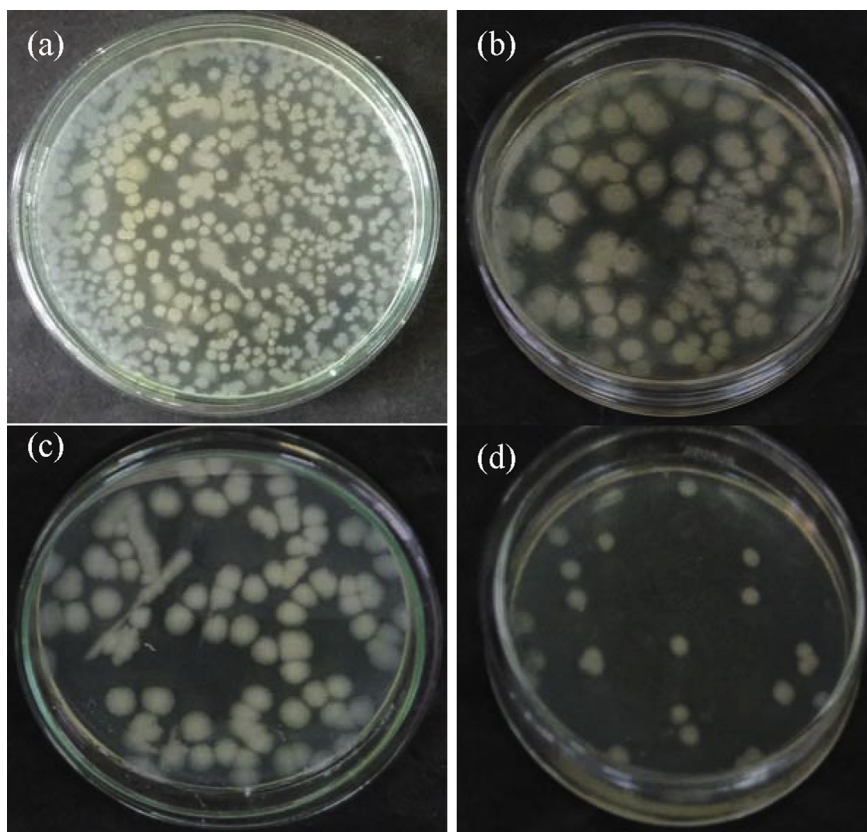


Figure 6: (a) Plate showing number of colonies of *Staphylococcus aureus* before treatment of AgNPs, (b) after 6 h of treatment with AgNPs, (c) after 10 h of treatment with AgNPs, (d) after 18 h of treatment with AgNPs.

measuring its intensity at 426 nm over two months. No significant change in the intensity was observed, which demonstrated its stability.

In FTIR spectra, the peak at 3440 cm^{-1} in the spectrum of AgNPs can be assigned to the —NH stretching of amines in the protein. The bands at approximately 2929 cm^{-1} and 2832 cm^{-1} can be attributed to C—H stretching of aromatic compounds. The dominant peak at approximately 1635 cm^{-1} can be assigned to C=O stretching of amide-I and amide-II, respectively, and should be regarded as the presence of the proteins.²⁸ The bands at approximately 1460 cm^{-1} and 1383 cm^{-1} can be attributed to C—H bending. The bands at 1243 cm^{-1} and 1055 cm^{-1} can be attributed to C—O stretching. The bands at 793 cm^{-1} and 605 cm^{-1} can be assigned to C—Cl stretching, which is characteristic of alkyl halides. It may be concluded from the FTIR spectroscopic study that the secondary structure of proteins in the *B. asiatica* extract are not affected because of their interaction with Ag^+ ions or nanoparticles and acts as the capping agents to the phytosynthesized AgNPs.²⁹ The results obtained from various characterization methods revealed that AgNPs were in the size range of 15 nm–35 nm and crystallized in face-centred-cubic structure. The corresponding electron diffraction pattern obtained by XRD analysis confirmed the “face-centred-cubic” crystalline structure of AgNPs. The average crystalline size of phytosynthesized AgNPs was calculated using Scherrer’s equation: $D = k\lambda / \beta \cos\theta$,³⁰ where D is the particle diameter size, k is a constant (equal to 0.9), λ is the wavelength of X-ray source (1.5406 \AA) and β is the full-width at half maximum (FWHM) of the XRD peak at the diffraction angle θ . The average calculated crystalline size of phytosynthesized AgNPs was approximately 27 nm. Silver (70.22%) was the major constituent element compared to copper (28.80%) and oxygen (0.89%). The EDS profile showed a strong signal for silver along with some peaks that may have originated from the biomolecules that are bound to the surface of AgNPs, indicating the reduction of silver ions to elemental silver.

Biofilm formation and bacterial infections on the surface of medical devices are a major concern worldwide and a serious challenge for biomedical science. Hence, topical applications of effective antibacterial agents are needed to reduce biofilm formation and infection. Despite antibiotic therapy, infection caused by Gram-positive pathogenic bacteria *S. epidermidis* and *S. aureus* are difficult due to the emergence of resistance to currently available antibiotics. Therefore, alternative antibacterial agents are needed for treatment of infections caused by these microorganisms and has prompted us to search for a suitable topical anti-infective agent. We focussed on preparations of an agent that reduces bacterial infection and biofilm formation while limiting drug resistance. In this study, phytosynthesized AgNPs have a potential application as a pathogenic biofilms growth inhibitor and may have future applications in the development of derivative agents to control the spread and infection of a wide range of drug resistant pathogenic strains.

Conclusions

In this study, we synthesized AgNPs from leaf extracts of *B. asiatica*. The synthesized AgNPs were spherical in shape

with size ranging from 15 nm to 35 nm, as observed in XRD, TEM and AFM analysis. We have demonstrated that phytosynthesized AgNPs capped with various functional groups of the adsorbed biomolecules coated on glass surface help prevent biofilm formation and adhesion of *S. epidermidis* and *S. aureus*. Thus, coating of phytosynthesized AgNPs on glass surfaces may provide efficient antibacterial agents in treating medical device associated infection of *S. epidermidis* prepared by *B. asiatica* leaf extracts. In spite of these findings, a greater understanding of biofilm formation may lead to better predictability of biofilm processes such as detachment, as well as more effective control strategies.

Conflict of interest

The authors have no conflict of interest to declare.

Authors’ contributions

As conceived and designed the study, conducted research, provided research materials, and collected and organized data. AS and KJ analysed and interpreted the data. KJ collected the plant material and synthesized the silver nanoparticles. KJ wrote initial and final draft of article, and provided logistic support. All authors have critically reviewed and approved the final draft and are responsible for the content and similarity index of the manuscript.

Acknowledgements

Authors gratefully acknowledge the necessary instrumental facilities, consumables and constant supervision provided by the Department of Biotechnology, Govind Ballabh Pant Engineering College, Pauri Garhwal, Uttarakhand, India. KJ is thankful to TEQIP-II (Technical Education Quality Improvement Program, a World Bank funded project) for providing fellowship.

References

1. Lu AH, Salabas EL, Schuth F. Magnetic nanoparticles: synthesis, protection, functionalization, and application. *Angew Chem Int Ed Engl* 2007; 46: 1222–1244.
2. De M, Ghosh PS, Rotello VM. Applications of nanoparticles in biology. *Adv Mater* 2008; 20: 4225–4241.
3. Ghosh PS, Rajib C. Core/shell nanoparticles: classes, properties, synthesis mechanisms, characterization, and applications. *Chem Rev* 2012; 112: 2373–2433.
4. Mallick K, Witcomb MJ, Scurell MS. Polymer stabilized silver nanoparticles: a photochemical synthesis route. *J Mater Sci* 2004; 39: 4459–4463.
5. Chandran SP, Chaudhary M, Pasricha R, Ahmed A, Sastry M. Synthesis of gold nanotriangles and silver nanoparticles using Aloe vera plant extract. *Biotechnol Prog* 2006; 22: 577–583.
6. Oluyomi SA, Temiloluwa OF. Antioxidant status of rats administered silver nanoparticles orally. *J Taibah Univ Med Sci* 2014; 9: 182–186.
7. Perni S, Callard PE, Prokopovich P. Success and failure of colloidal approached in bacterial adhesion. *Adv Colloid Interf Sci* 2014; 206: 265–274.
8. Otto M. *Staphylococcus epidermidis*- the ‘accidental’ pathogen. *Nat Rev Microbiol* 2009; 7: 555–567.

9. Uckay I, Pittet D, Vaudoaux P, Sax H, Lew D. Foreign body infections due to *Staphylococcus epidermidis*. **Ann Med** 2009; 41: 109–119.
10. Costerton JW, Stewart PS, Greenberg EP. Bacterial biofilms: a common cause of persistent infections. **Science** 1999; 284: 1318–1322.
11. Costerton W, Veeh R, Shirtliff M, Pasmore M, Post C, Ehrlich G. The application of biofilm science to the study and control of chronic bacterial infections. **J Clin Invest** 2003; 112: 1466–1477.
12. Rohde H, Mack D, Christner M, Burdelski C, Franke G, Knobloch JKM. Pathogenesis of staphylococcal device-related infections: from basic science to new diagnostic, therapeutic and prophylactic approaches. **Rev Med Microbiol** 2006; 17: 45–54.
13. Saravanan M, Vemu AK, Barik SK. Rapid biosynthesis of silver nanoparticles from *Bacillus megaterium* (NCIM 2326) and their antibacterial activity on multi drug resistant clinical pathogens. **Colloids Surf B** 2011; 88: 325–331.
14. Bal KE, Bal Y, Cote G, Chagnes A. Morphology and antimicrobial properties of *Luffa cylindrica* fibers/chitosan biomaterial as micro-reservoirs for silver delivery. **Mater Lett** 2012; 79: 238–241.
15. Nadworny PL, Wang J, Tredget EE, Burrell RE. Anti-inflammatory activity of nanocrystalline silver in a porcine contact dermatitis model. **Nanomedicine** 2008; 4: 241–251.
16. Gurunathan S, Lee KJ, Kalishwaralal K, Sheikpranbabu S, Vaidyanathan R, Eom SH. Antiangiogenic properties of silver nanoparticles. **Biomaterials** 2009; 30: 6341–6350.
17. Tan H, Peng Z, Li Q, Xu X, Guo S, Tang T. The use of quaternised chitosan-loaded PMMA to inhibit biofilm formation and down regulate the virulence-associated gene expression of antibiotic-resistant *Staphylococcus*. **Biomaterials** 2012; 33: 365–377.
18. Nuryastuti T, Van der Mei HC, Busscher HJ, Irvati S, Aman AT, Krom BP. Effect of cinnamon oil on *icaA* expression and biofilm formation by *Staphylococcus epidermidis*. **Appl Environ Microbiol** 2009; 75: 6850–6855.
19. König DP, Schierholz JM, Hilgers RD, Bertram C, Perdreau-Remington F, Rutt J. In vitro adherence and accumulation of *Staphylococcus epidermidis* RP62A and *Staphylococcus epidermidis* M7 on four different bone cements. **Langenbecks Arch Surg** 2001; 386: 328–332.
20. Thakur RS, Puri HS, Akhtar H. *Major medicinal plants of India*. Lucknow: Central Institute of Medicinal and Aromatic Plants; 1980. p. 114.
21. Pandey G. *Medicinal plants of Himalaya*. Delhi: Sri Satguru Publication; 2000. pp. 68–69.
22. Jyoti K, Baunthiyal M, Singh A. Characterization of silver nanoparticles synthesized using *Urtica dioica* Linn. leaves and their synergistic effects with antibiotics. **J Radiat Res Appl Sci** 2016; 9: 217–227.
23. Pallavicini P, Taglietti A, Dacarro G, Diaz-Fernandez G, Galli YA, Grisoli M, Patrini P, Santucci De Magistris MG, Zanoni R. Self-assembled monolayers of silver nanoparticles firmly grafted on glass surfaces: low Ag⁺ release for an efficient antibacterial activity. **J Colloid Interface Sci** 2010; 350: 110–116.
24. Rocha TCR, Winnischofer H, Westphal E, Zanchet D. Formation kinetics of silver triangular nanoplates. **J Phys Chem C** 2007; 111: 2885.
25. Shah A, Rahman L, Qureshi R, Rehman Z. Synthesis, characterization, and application of Au–Ag alloy nanoparticles for the sensing of an environmental toxin pyrene. **Rev Adv Mater Sci** 2012; 30: 133.
26. Kaviya S, Santhanalakshmi J, Viswanathan B, Muthumar J, Srinivasan K. Green synthesis of silver nanoparticles using *Polyalthia longifolia* leaf extracts along with D-sorbitol: study of antibacterial activity. **Spectrochim Acta A Mol Biomol Spectrosc** 2011; 79: 594–598.
27. Zaheer Z, Rafiuddin. Silver nanoparticles to self assembled films: green synthesis and characterization. **Colloids Surf B** 2012; 90: 48–52.
28. Prakash P, Gnanaprakasam P, Emmanuel R, Arokiyaraj S, Saravanan M. Green synthesis of silver nanoparticles from leaf extract of *Mimusops elengi*, Linn. for enhanced antibacterial activity against multi drug resistant clinical isolates. **Colloids Surf B** 2013; 108: 255–259.
29. Niraimathi KL, Sudha V, Lavanya R, Brindha P. Biosynthesis of silver nanoparticles using *Alternanthera sessilis* (Linn.) extract and their antimicrobial, antioxidant activities. **Colloids Surf B** 2013; 102: 288–291.
30. Dubey SP, Lahtinen M, Sillanpää M. Tansy fruit mediated greener synthesis of silver and gold nanoparticles. **Process Biochem** 2010; 45: 1065–1071.

How to cite this article: Jyoti K, Singh A. Evaluation of antibacterial activity from phytosynthesized silver nanoparticles against medical devices infected with *Staphylococcus* spp. **J Taibah Univ Med Sc** 2017;12(1):47–54.